Available online at www.sciencedirect.com
SCIENCE DIRECT®
Graphical Models 68 (2006) 237–254
Graphical Models
www.elsevier.com/locate/gmod

Manifold splines

Xianfeng Gu, Ying He *, Hong Qin

Center for Visual Computing (CVC), Department of Computer Science, Stony Brook University, Stony Brook, NY 11794-4400, USA

Received 21 February 2005; received in revised form 1 December 2005; accepted 6 March 2006

Abstract

Constructing splines whose parametric domain is an arbitrary manifold and effectively computing such splines in real-world applications are of fundamental importance in solid and shape modeling, geometric design, graphics, etc. This paper presents a general theoretical and computational framework, in which spline surfaces defined over planar domains can be systematically extended to manifold domains with arbitrary topology with or without boundaries. We study the affine structure of domain manifolds in depth and prove that the existence of manifold splines is equivalent to the existence of a manifold's affine atlas. Based on our theoretical breakthrough, we also develop a set of practical algorithms to generalize triangular *B*-spline surfaces from planar domains to manifold domains. We choose triangular *B*-splines mainly because of its generality and many of its attractive properties. As a result, our new spline surface defined over any manifold is a piecewise polynomial surface with high parametric continuity without the need for any patching and/or trimming operations. Through our experiments, we hope to demonstrate that our novel manifold splines are both powerful and efficient in modeling arbitrarily complicated geometry and representing continuously varying physical quantities defined over shapes of arbitrary topology.

Keywords: Geometric modeling; Manifold spline; Riemann surface; Conformal structure; Affine atlas

1. Introduction and motivation

Real-world volumetric objects are oftentimes of complex geometry and arbitrary topology. One fundamental goal of solid and physical modeling is to seek accurate and effective techniques for the compact representation of smooth shapes with applications in both scientific research and industrial practice. Towards this goal, subdivision surfaces have been extensively investigated during the recent past. Despite their modeling advantages for arbitrarily complicated geometry and topology, subdivision surfaces have two drawbacks: (1) accurate surface evaluation is frequently conducted via explicit, recursive subdivision since most subdivision schemes (especially those interpolatory schemes) do not allow closed-form analytic formulation for their basis functions; (2) extraordinary points depend on the connectivity of the control mesh and need special care, as their behaviors and smoothness properties differ significantly from other regular regions nearby. This paper aims to tackle the aforementioned technical challenges associated with popular subdivision surfaces by articulating

* Corresponding author.
E-mail address: yhe@cs.sunysb.edu (Y. He).

1524-0703/$ - see front matter © 2006 Elsevier Inc. All rights reserved.
doi:10.1016/j.gmod.2006.03.004

the new theory for manifold splines and developing novel algorithms for constructing such splines in practice.

Aside from subdivision surfaces, this research is equally motivated by the rigorous mathematics of spline theory. Spline surfaces have demonstrated their significance in shape modeling, finite element analysis, scientific computation, visualization, manufacturing, etc. Most popular examples include Bézier surfaces, tensor-product *B*-spline surfaces, and triangular *B*-spline surfaces. Essentially, all of them are piecewise polynomials defined over planar parametric domains for efficient evaluation. While these spline surfaces are ideal for modeling open surfaces with curved boundaries, they are cumbersome to represent smooth surfaces with arbitrarily complex topology. The feasible way is to trim parametric spline surfaces defined over open planar domains, stitch them along their trimmed edges with care, and enforce the continuity requirements of certain degree across their shared boundaries as shown in [1]. It is challenging to maintain high order continuity across patches in both theory and practice. Therefore, there is a pressing need to introduce the new spline concept and develop the new spline theory that define polynomial splines over arbitrary manifold without trimming and stitching operations.

In essence, constructing splines defined over arbitrary manifolds is of fundamental significance in geometric design, and interactive graphics. This paper presents a general theoretical framework that can systematically generalize spline surfaces with planar domains to manifold domains with arbitrary topology with or without boundaries. The specific contributions of this paper include:

- While motivated by the above observations, it also significantly advances the state-of-the-art of both subdivision surfaces and splines surfaces.
- This paper gives a theoretical proof for the existence of manifold splines, i.e., it is equivalent to the existence of the affine structure of the underlying manifold serving as a parametric domain.
- Classical characteristic class theory has concluded that no closed surface admits an affine atlas except tori, so it provides evidence that the existence of extraordinary points depends only on topology.
- Besides the theoretical advances, this paper also devises a set of practical algorithms that enable the effective modeling of triangular *B*-spline surfaces over manifold domains. The resulting surface is a piecewise polynomial surface with high parametric continuity without any patching or trimming operations.
- Due to the intrinsic topological obstructions associated with domain manifolds, the manifold triangular *B*-spline still admits singular points (which can not be evaluated by the new spline scheme). However, our modeling algorithms are able to construct the manifold spline based on triangular *B*-splines with the minimum number of singular points. This lower bound results from Riemann surface theory (e.g., conformal structure).

In this paper, we choose to work on triangular *B*-splines and their manifold generalization, mainly because triangular *B*-splines have many important properties:

- Triangular *B*-spline surfaces are defined over arbitrary planar triangulations, and they generalize tensor-product *B*-splines. Unlike tensor-product *B*-splines, it has no strict requirements for connectivity of the underlying mesh domain.
- Local support, parametric affine invariance, the completeness of basis functions, and polynomial reproduction are attractive properties for triangular *B*-splines, and they still hold when generalizing to manifold splines.
- Triangular *B*-splines exhibit the maximal order of continuity with the lowest possible degree of their basis functions. For example, they achieve C^2 continuity when using only cubic polynomials. Furthermore, spatially varying smoothness requirements and sharp features can easily be achieved via different knot placements in the parametric domain.

With our new results shown in this paper, it is rather straightforward to generalize other popular splines to their manifold counterparts by adopting our techniques on triangular *B*-splines. It may be noted that the new triangular *B*-splines defined over arbitrary manifolds may still have special, singular points which must require separate, additional care (Note that singular points for manifold splines differ from extraordinary points of subdivision surfaces, where the vertex valence is the only criterion). The intrinsic reason for the existence of singular points (when using manifold splines) is due to the topological obstruction of the underlying domain. In principle, an arbitrary domain can not offer a special atlas such that all transition

functions are affine. In practice, however, by removing a finite number of points, the domain will then admit the affine atlas and subsequently allow the meaningful generalization of triangular *B*-splines to arbitrary manifolds.

After the problem statement and its motivation, the remainder of this paper is organized as follows. Section 2 briefly reviews the prior work. Section 3 presents the necessary mathematical tools for manifold splines. Section 4 documents the theoretical foundation of our novel manifold splines. Section 5 explains the algorithmic details for constructing triangular *B*-splines over arbitrary manifold. Section 6 discusses the implementation issues and presents our experimental results. Finally, we conclude the paper and briefly discuss the future research in Section 7.

2. Prior work

This section briefly surveys some related work in triangular *B*-splines and surfaces defined on manifolds.

2.1. Triangular B-splines

The theoretical foundation of triangular *B*-splines lies in the multivariate *B*-spline, or simplex spline, introduced by de Boor [2]. It has received much attention since its inception. Dahmen et al. [3] propose triangular *B*-splines from the point of view of blossoming, which offers a general scheme for constructing a collection of multivariate *B*-splines (with $n-1$ continuous derivatives) whose linear span comprises all polynomials of degree at most n. Fong and Seidel [4] present the first prototype implementation of triangular *B*-splines and show several useful properties, such as affine invariance, convex hull, locality, and smoothness. Greiner and Seidel [5] show the practical feasibility of multivariate *B*-spline algorithms in graphics and shape design. Pfeifle and Seidel [6] demonstrate the fitting of a triangular *B*-spline surface to scattered functional data through the use of least squares and optimization techniques. Franssen et al. [7] propose an efficient evaluation algorithm, which works for triangular *B*-spline surfaces of arbitrary degree. Neamtu [8] describes a new paradigm of bivariate simplex splines based on the higher degree Delaunay configurations. He et al. [9] present an efficient method to fair triangular *B*-spline surfaces of arbitrary topology.

2.2. Spherical splines

Traditional *B*-splines are defined on planar domains. Many researchers have explored the feasible ways to generalize splines to be defined on sphere and manifolds with arbitrary topology. We only document a few of them in the interest of space.

Defining splines over a sphere has been studied during the past decade. Alfeld et al. [10] present spherical barycentric coordinates which naturally lead to the theory of Spherical Bernstein–Bézier polynomials (SBB). They show fitting scattered data on sphere-like surfaces with SBB in [11]. Pfeifle and Seidel [12] present scalar spherical triangular splines and demonstrate the use of these splines for approximating spherical scattered data. Neamtu [13] constructs a functional space of homogeneous simplex splines and shows that restricting the homogeneous splines to a sphere gives rise to the space of spherical simplex splines. He et al. [14] present rational spherical spline for genus zero shape modeling.

2.3. Surfaces defined on manifolds

There are some related work on defining functions on manifold, such as [15–19]. These methods share similar construction procedures which can be summarized as follows:

(1) Find an atlas $\{U_i, \phi_i\}$ to cover the domain manifold M, with transition functions $\phi_{ij} = \phi_j \circ \phi_i^{-1}$. All transition functions are required to be smooth, especially, analytical functions are used in [19].
(2) Define functional basis on each chart $f_i{:}\phi_i(U_i) \to R$.
(3) For each point $p \in M$, normalize these functions and define the basis functions B_i as

$$B_i(p) = \frac{f_i(p)}{\sum_j f_j(p)}.$$

(4) Define the functions as $F(p) = \sum_i C_i B_i(p)$ where C_i are the control points.

It is obvious that, even when B_i is a polynomial on chart (U_i, ϕ_i), B_i is *not* a polynomial on a different overlapping chart (U_j, ϕ_j), because in general ϕ_{ij} is NOT algebraic and $\phi_{ij} \circ B_i$ is not a polynomial.

Our work is completely different from the above work in that: (1) The transition functions of our method must be affine. Therefore, the requirement

of our method is much stronger. That is why topological obstruction plays an important role in our construction. (2) Our method produces the polynomial or rational polynomials. On any chart, the basis functions are always polynomials or rationals, and represented as *B*-splines or rational *B*-splines.

A different approach using the concept of orbifold is introduced in [20]. Suppose S is the domain manifold with genus g and without boundaries. Then, the universal covering space $\tilde{S}$ can be embedded in either a sphere, a plane or hyperbolic space. If the transformation group H of $\tilde{S}$ maps a fundamental domain to a fundamental domain, then the spline surface is defined on $\tilde{S}$ with the unique requirement that the spline is invariant under H. They embed the sphere and the hyperbolic space in $\mathbb{R}^3$ and define the spline on $\mathbb{R}^3$ directly. Our method is fundamentally different. First, we define the splines on the atlas of S, not on the universal covering space $\tilde{S}$. Second, each local parameter is only 2D instead of 3D. Third, our construction is intrinsic to the surface S; namely, we do not need any embedding information. Fourth, their method can also be considered as building an atlas, where each chart is a subset in $\mathbb{R}^3$ and the transition functions are non-linear. In contrast, our method constructs an atlas where each chart is an open set in $\mathbb{R}^2$ and all transition functions are affine.

In summary, we believe manifold splines have two fundamental criteria:

(1) Manifold: the splines are defined on the domain manifold, namely, the evaluation of the splines is *independent* of the choice of the chart.
(2) Algebraic: locally, on any chart, the splines should be either *polynomials or rational polynomials*.

All previous manifold constructions focus on the first point but can not satisfy the second one. Most spline schemes emphasize the algebraic aspect, but only are defined on planar domains. Our work is the first one that satisfies both criteria, and discovers the intrinsic relation between manifold splines and affine structures.

3. Theoretical background

To define splines on manifolds, we must fully understand the intrinsic properties of splines and the special structures inherent to the domain manifold. This section presents the relevant theoretical tools.

Essentially, splines have local support, so we shall define spline patches locally on the manifold and glue the locally defined spline patches to cover the entire domain manifold. Furthermore, since splines are invariant under parametric affine transformations, we seek to glue the patches using affine transition functions. Therefore, if the domain surface admits an atlas on which all transition functions are affine, then we can glue the patches coherently. However, the existence of such an atlas is solely determined by the topology. In principle, we can glue the patches to cover the entire surface except a finite number of points, which are singular points and can not be evaluated by the global splines on the manifold. These singular points represent the topological obstruction for the existence of the affine atlas.

3.1. Spline theory and properties

The most popular spline schemes, such as tensor product Bézier surfaces, tensor product *B*-spline surfaces, triangular Bézier surfaces and *B*-patches, can be unified as the different variations of polar forms [21–23]. We shall briefly explain the concept of polar forms, and then, we concentrate on *B*-patches and triangular *B*-spline surfaces, because of their flexibility and generality.

3.1.1. Polar form

In essence, a polar form is a multivariate polynomial that is symmetric and multi-affine.

Definition 1 (*Affine map*)**.** A map $f : \mathbb{R}^2 \to \mathbb{R}^n$ is affine, if and only if it preserves affine combinations, i.e., if and only if $f(\sum_{i=0}^{m} \alpha_i \mathbf{u}_i) = \sum_{i=0}^{m} \alpha_i f(\mathbf{u}_i)$ whenever $\sum_{i=0}^{m} \alpha_i = 1$.

Definition 2 (*Symmetric*, *multi-affine*)**.** Let F be an n-variable map. F is symmetric if and only

$$F(\mathbf{u}_1, \mathbf{u}_2, \ldots, \mathbf{u}_n) = F(\mathbf{u}_{\pi(1)}, \mathbf{u}_{\pi(2)}, \ldots, \mathbf{u}_{\pi(n)})$$

for all permutations $\pi \in \sum_n$. The map F is multi-affine if and only if F is affine in each argument if the others are held fixed.

The well-known blossoming principle indicates that any polynomial is equivalent to its polar form.

Proposition 3. *Polynomials $F : \mathbb{R}^2 \to \mathbb{R}^t$ of degree n, and a symmetric multi-affine map $f : (\mathbb{R}^2)^n \to \mathbb{R}^t$ are equivalent. Given a map of either type, unique map of the other type exists that satisfies the identity*

$F(\mathbf{u}) = f(\underbrace{\mathbf{u},\ldots,\mathbf{u}}_{n})$. *The map f is called the multi-affine polar form or blossom of F.*

3.1.2. B-patches and triangular B-splines

Triangular B-spline surfaces can be defined on planar domains with arbitrary triangulations. In particular regions, triangular B-splines are B-patches. For the convenience, we introduce notations which are similar to those employed in [3,24]. Essentially, we formulate B-patches through the use of a polar form. Let $\Delta^I := [\mathbf{t}^I_0, \mathbf{t}^I_1, \mathbf{t}^I_2]$ be the triangle "I" of our triangulation $\mathscr{T}$ of $\mathbb{R}^2$. For each vertex $\mathbf{t}^I_i$ we assign a list of $k+1$ distinct additional knots

$$\mathbf{t}^I_i := \{\mathbf{t}^I_{i,0}, \mathbf{t}^I_{i,1}, \ldots, \mathbf{t}^I_{i,k}\}. \tag{1}$$

The rule proposed in [3] consists of producing a subset V^I_β, where $\beta = (\beta_0, \beta_1, \beta_2)$ are three non-negative integers, as follows:

$$V^I_\beta := \{\mathbf{t}^I_{0,0}, \mathbf{t}^I_{0,1}, \ldots, \mathbf{t}^I_{0,\beta_0}, \mathbf{t}^I_{1,0}, \mathbf{t}^I_{1,1}, \ldots, \mathbf{t}^I_{1,\beta_1}, \mathbf{t}^I_{2,0}, \mathbf{t}^I_{2,1}, \ldots, \mathbf{t}^I_{2,\beta_2}\}.$$

If we want to define a degree k simplex splines, we must impose that

$$|\beta| := \beta_0 + \beta_1 + \beta_2 = k.$$

V^I_β is the set of all knots associated with one vertex in $\mathscr{T}$.

We further define $\Delta^I_\beta := [\mathbf{t}^I_{0,\beta_0}, \mathbf{t}^I_{1,\beta_1}, \mathbf{t}^I_{2,\beta_2}]$ and

$$\begin{aligned} X^I_\beta :& \\ &= (\mathbf{t}^I_{0,0}, \ldots, \mathbf{t}^I_{0,\beta_0-1}, \mathbf{t}^I_{1,0}, \ldots, \mathbf{t}^I_{1,\beta_1-1}, \mathbf{t}^I_{2,0}, \ldots, \mathbf{t}^I_{2,\beta_2-1}) \\ &\in (\mathbb{R}^2)^{|\beta|}. \end{aligned} \tag{2}$$

X^I_β is the set of knots associated with one control point $f(X^I_\beta)$.

If Δ^I_β is non-degenerate, it is possible to define the barycentric coordinates of $\mathbf{u} \in \mathbb{R}^2$ with respect to this triangle

$$\mathbf{u} = \sum_{i=0}^{2} \lambda^I_{\beta,i}(\mathbf{u})\mathbf{t}^I_{i,\beta_i} \text{ and } \sum_{i=0}^{2} \lambda^I_{\beta,i}(\mathbf{u}) = 1. \tag{3}$$

The generalized algorithm computes $F(\mathbf{u})$ starting from the values $f(X^I_\beta)$, $|\beta| = k$. Those values are called the *poles* of F. Let us define

$$X^I_\beta \mathbf{u}^v := X^I_\beta \times (\underbrace{\mathbf{u},\mathbf{u},\ldots,\mathbf{u}}_{v}) \in (\mathbb{R}^2)^{|\beta|+v}$$

and assign $C^v_\beta(\mathbf{u}) := f(X^I_\beta \mathbf{u}^v)$ with $|\beta| = k - v$, the algorithm uses the k-affinity of f stating the recurrence relation:

$$C^0_\beta(\mathbf{u}) := f(X^I_\beta), |\beta| = k,$$

$$C^{v+1}_\beta(\mathbf{u}) := \sum_{i=0}^{2} \lambda^I_{\beta,i}(\mathbf{u}) C^v_{\beta+e^i}(\mathbf{u}), \tag{4}$$

where e^i denotes the canonical basis vector. Then $F(\mathbf{u}) = C^k_0(\mathbf{u})$. If the basis function for the pole $f(X^I_\beta)$ is denoted as $B^I_\beta(\cdot)$, then we obtain

$$F(\mathbf{u}) = \sum_{|\beta|=k} f(X^I_\beta) B^I_\beta(\mathbf{u}).$$

3.1.3. Triangular B-spline properties

Triangular B-splines have the following valuable properties which are critical for geometric and solid modeling:

(1) *Local support.* The spline surface has local support. To evaluate the image $F(\mathbf{u})$ of a point $\mathbf{u} \in \Delta^I$, we only need control points $\mathbf{c}^J_\beta$ (associated with knot set V^J_β on triangle J), where triangle J belongs to the 1-ring neighborhood of triangle I.
(2) *Convex hull.* The polynomial surface is completely inside the convex hull of the control points.
(3) *Completeness.* The B-spline basis is complete, namely, a set of degree n B-spline basis can represent any polynomial with degree no greater than n via a linear combination.
(4) *Parametric affine invariance.* The choice of parameter is not unique: if one transforms the parameter affinely and the corresponding knots of control points are transformed accordingly, then the polynomial surface remains unchanged (see Fig. 1).
(5) *Affine invariance.* If the control net is transformed affinely, the polynomial surface will be consistently transformed affinely.

Note that parametric affine invariance is different from affine invariance. The diagrams below illustrate the radical difference.

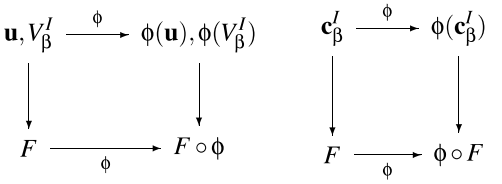

(a) Parametric affine invariance (b) Affine invariance

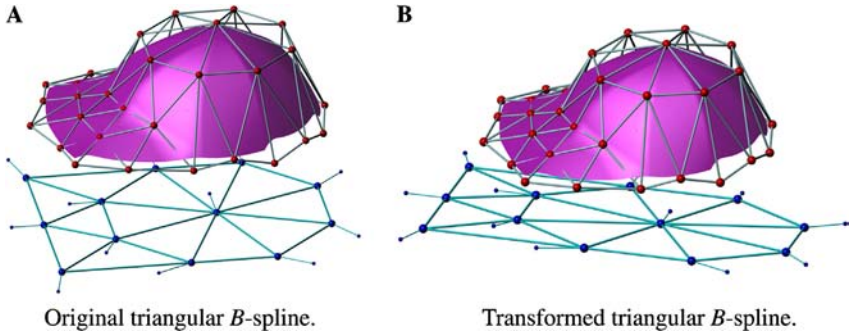

Fig. 1. Parametric affine invariance: (A and B) are two triangular *B*-splines sharing the same control net, the two parametric domains differ only by an affine transformation. The same control nets result in the same polynomial surfaces shown in (A and B). (Spline model courtesy of M. Franssen.)

The left one above represents parametric affine invariance, which refers to the property that, under a transformation between parameter domains, the shape of the polynomial surface remains the same; the right one above indicates affine invariance, which refers to the property that under a transformation of the control points, the polynomial surface will change accordingly.

The aforementioned properties are extremely important for geometric and solid modeling applications. For example, the local support will allow designers to adjust the surface by moving nearby control points without affecting the global shape. Therefore, it is crucial to preserve these properties when we generalize the planar domain *B*-splines to manifold *B*-splines. We will prove that such a generalization does exist, and these desirable properties can be preserved. The generalization completely depends on the so-called affine structure of the domain manifold. The local support and parametric affine invariance are crucial for constructing manifold splines.

3.2. Manifold and geometric structures

Our manifold splines are defined over manifolds with arbitrary topology with or without boundaries. An n dimensional manifold can be treated as a set of open sets in $\mathbb{R}^n$ glued coherently (see Fig. 2).

Definition 4 (*Manifold*)**.** A manifold of dimension n is a connected Hausdorffff space M for which every point has a neighborhood U that is homeomorphic to an open subset V of $\mathbb{R}^n$. Such a homeomorphism

$$\phi : U \to V$$

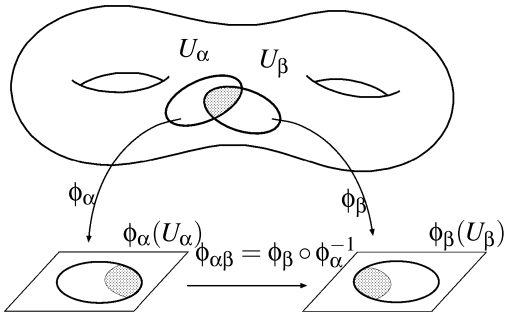

Fig. 2. Manifold: the manifold is covered by a set of charts (U_α, ϕ_α), where $\phi_\alpha : U_\alpha \to \mathbb{R}^2$. If two charts (U_α, ϕ_α) and (U_β, ϕ_β) overlap, the transition function $\phi_{\alpha\beta} : \mathbb{R}^2 \to \mathbb{R}^2$ is defined as $\phi_{\alpha\beta} = \phi_\beta \circ \phi_\alpha^{-1}$.

is called a coordinate chart. An *atlas* is a family of charts $\{(U_\alpha, \phi_\alpha)\}$ for which U_α constitute an open covering of M.

Transition function plays a vital role in the theory of manifold splines.

Definition 5 (*Transition function*)**.** *Suppose* $\{(U_\alpha, \phi_\alpha)\}$ *and* $\{(U_\beta, \phi_\beta)\}$ *are two overlapping charts on a manifold* M, $U_\alpha \cap U_\beta \neq \emptyset$, *the chart transition is*

$$\phi_{\alpha\beta} : \phi_\alpha(U_\alpha \cap U_\beta) \to \phi_\beta(U_\alpha \cap U_\beta)$$

Transition functions satisfy the cocycle condition (see Fig. 3)

$$\phi_{\alpha\beta} \circ \phi_{\beta\gamma} = \phi_{\alpha\gamma}, \quad \forall x \in U_{\alpha\beta} \cap U_{\beta\gamma}.$$

Atlas can be classified by transition functions.

Definition 6 (*Geometric structure*)**.** Suppose M is a manifold, X is a topological space, G is a transformation group on X, a (G, X) *atlas* is an atlas $\{(U_\alpha, \phi_\alpha)\}$, such that

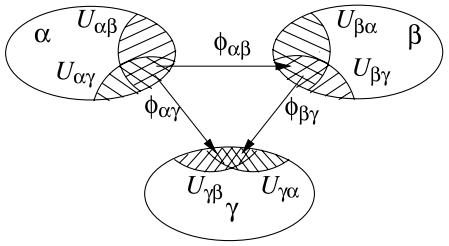

Fig. 3. Cocycle condition for transition functions.

(1) Local coordinates are in X

$\phi_\alpha : U_\alpha \to X$.

(2) Transition functions are in group G

$\phi_{\alpha\beta} \in G$.

Two (G, X) atlas are equivalent, if their union is still a (G, X) atlas. Each equivalent class of (G, X) atlas is a (G, X) structure.

Genus zero closed surfaces have spherical structure. Genus one surfaces have Euclidean structure. Surfaces with high genus have hyperbolic structure. Surfaces have general geometric structures, such as conformal structure, projective structure. Table 1 illustrates the common geometric structures (Fig. 4).

3.3. Affine structure

An affine manifold is a manifold with special transition functions.

Definition 7. A two-dimensional manifold M with an atlas $\{(U_\alpha, \phi_\alpha)\}$, if all chart transition functions

$$\phi_{\alpha\beta} := \phi_\beta \circ \phi_\alpha^{-1} : \phi_\alpha(U_\alpha \bigcap U_\beta) \to \phi_\beta(U_\alpha \bigcap U_\beta)$$

are affine, then the atlas is called an affine atlas, M is called an affine manifold.

Two affine atlases are *equivalent* if their union is still an affine atlas. All the equivalent affine atlases form an *affine structure* of the manifold.

For closed surfaces, only genus-one surfaces have affine structures (see Fig. 2), but all surfaces with boundaries have affine structures. Next, in order to construct affine atlas for general surfaces in practice, we need certain theoretical tools which are induced from the *conformal structure* of the domain manifold.

3.4. Conformal structure

Similar to affine structure, conformal structure is also an intrinsic structure of the surface. A conformal atlas is an atlas such that all transition

Table 1
General geometric structures

Structure	X	G	Surfaces
Topology	$\mathbb{R}^2$	Homeomorphisms	Surfaces of arbitrary topology
Differential	$\mathbb{R}^2$	Diffeomorphisms	Surfaces of arbitrary topology
Spherical	$\mathbb{S}^2$	Rotation	Closed, genus zero surfaces
Euclidean	$\mathbb{E}^2$	Rigid motion	Closed, genus one surfaces
Hyperbolic	$\mathbb{H}^2$	Möbius Transformation	High genus surfaces
Affine	$\mathbb{R}^2$	Affine transformation	Zero Euler class surfaces
Conformal	$\mathbb{C}$	Holomorphic functions	Oriented surfaces of arbitrary topology
Projective	$\mathbb{RP}^2$	Projective Transformation	Oriented surfaces of arbitrary topology

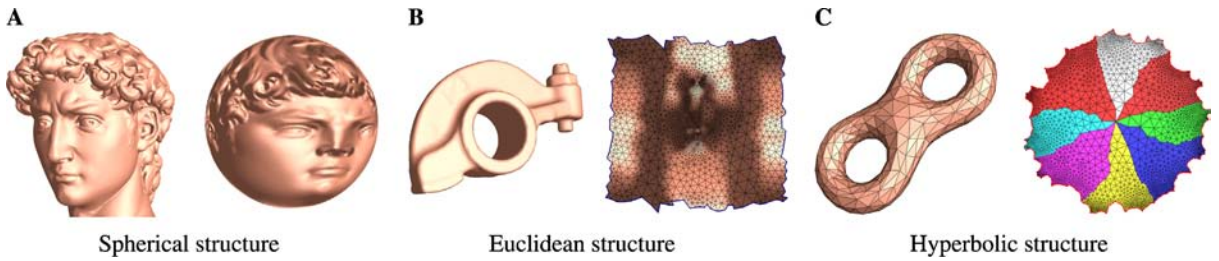

Fig. 4. Geometric structures. (A) Spherical structure: X is the unit sphere $\mathbb{S}^2$, G is the rotation group; (B) Euclidean structure: X is the Euclidean plane $\mathbb{R}^2$, G is the translation group; (C) hyperbolic structure: X is the hyperbolic space $\mathbb{H}^2$, G is the Möbius transformation group.

functions are conformal (analytic). Two conformal atlases are compatible if their union is still a conformal atlas. All compatible conformal atlases form conformal structure. All surfaces have conformal structure and are called Riemann surfaces [25]. Conformal structure is closely related to affine structure. In particular, an affine atlas can be computed by using special differential complex forms defined on the conformal atlas.

3.4.1. Riemann surface

The Riemann surface is a surface with a conformal atlas, such that all transition functions are analytic.

Definition 8 (*Analytic function*)**.** A function $f:\mathbb{C}\to\mathbb{C},(x,y)\to(u,v)$ is analytic, if it satisfies the following Riemann–Cauchy equation:

$$\frac{\partial u}{\partial x}=\frac{\partial v}{\partial y},\frac{\partial u}{\partial y}=-\frac{\partial v}{\partial x}$$

Definition 9 (*Riemann surface*)**.** A Riemann surface M is a 2-manifold with an atlas $\mathscr{A}=\{(U_\alpha,\phi_\alpha)\}$, such that all transition functions $\phi_{\alpha\beta}:\mathbb{C}\to\mathbb{C}$ are analytic. All compatible affine atlas forms a conformal structure of M.

Analytic functions are *conformal*, which intuitively means *angle preserving*. It is well known that all oriented metric 2 manifolds are Riemann surfaces and have a unique conformal structure, such that on each chart U_α,ϕ_α, the first fundamental form can be represented as $\mathrm{d}s^2=\lambda(u,v)(\mathrm{d}u^2+\mathrm{d}v^2)$. Gu and Yau [26,27] introduce practical algorithms to compute this conformal structure on general triangular meshes.

3.4.2. Holomorphic 1-form

To find an affine atlas, we need special differential forms defined on the conformal structure.

Definition 10 (*Holomorphic 1-form*)**.** Given a Riemann surface M with a conformal structure $\mathscr{A}$, a holomorphic 1-form ω is a complex differential form, such that on each local chart $(U,\phi)\in\mathscr{A}$

$$\omega=f(z)\,\mathrm{d}z, \tag{5}$$

where $f(z)$ is an analytic function, $z=u+\mathrm{i}v$ is the local parameter in the complex form.

Genus zero surface has no holomorphic 1-forms. The holomorphic 1-forms of closed genus g surface form a g complex dimensional linear space, denoted as $\Omega(M)$. A conformal atlas can be constructed by using a basis of $\Omega(M)$. This is the method derived in [26,27]. Considering its geometric intuition, a holomorphic 1-form can be visualized as two vector fields $\omega=(\omega_x,\omega_y)$, such that the curlex of ω_x and ω_y equals zero. Furthermore, one can rotate ω_x about the normal by a right angle to arrive at ω_y

$$\nabla\times\omega_x=0,\quad \nabla\times\omega_y=0,\quad \omega_y=n\times\omega_x.$$

By integrating a holomorphic 1-form, an affine atlas can be easily constructed. Figs. 11A and 8A illustrate holomorphic 1-forms on surfaces. The texture coordinates are obtained by integrating the 1-form on the surface (see [27] for the details).

3.4.3. Singular points

According to Poicaré–Hopf theorem, any vector field on a surface with nonzero Euler number must have singularities where the vector field is zero. Such singularities of $\omega=(\omega_x,\omega_y)$ are called *zero points*.

Definition 11 (*Zero point*). Given a Riemann surface M with a conformal structure $\mathscr{A}$, a holomorphic one-form ω, $\omega=f(z)\,\mathrm{d}z$, where $f(z)$ is an analytic function and $z=u+\mathrm{i}v$ is the local parameter. If at point p, $f(z)$ equals zero, p is a zero point of ω.

In fact, it can be proven that zero points do not depend on the choice of the local chart at all. For a Riemann surface M with genus g, a holomorphic 1-form ω has $2g-2$ zero points in principle. Zero points are singular points for our manifold splines (to be constructed later). Fig. 8A demonstrates the zero points (singular points) on the 1-form. The centers of regions with octagons are the zero points (Fig. 5).

4. Manifold spline theory

In this section, we will systematically define manifold splines using our theoretical results on affine structure and triangular *B*-splines and show their existence is equivalent to that of affine structure. We first discuss the existence of affine structure for general manifolds, and then we compute the affine structure through the use of conformal structure for any manifold. For the consistency of our manifold spline theory, we shall utilize the parametric affine invariance and polynomial reproduction properties of general spline schemes (triangular *B*-splines in particular for this paper).

Fig. 5. All oriented metric surfaces are Riemann surfaces which admit conformal structure.

4.1. Definition and concept

A manifold spline is geometrically constructed by gluing spline patches in a coherent way, such that the patches cover the entire manifold. The knots and control points are also defined consistently across the patches and the surface evaluation is independent of the choice of chart. First of all, we define the local spline patch. After that, we define a global manifold spline which can be decomposed into a collection of local spline patches.

Definition 12 (*Spline surface patch*)**.** A degree k spline surface patch is a triple $S = (U, C, F)$, where $U \subset \mathbb{R}^2$ is a planar simply connected parametric domain. $F : U \to \mathbb{R}^3$ is a piecewise polynomial surface and C is the set of control points, $C := \{\mathbf{c}^I_\beta, X^I_\beta \in (\mathbb{R}^2)^{|\beta|}, |\beta| = k\}$. F can be evaluated from C by polar form.

Definition 13 (*Manifold spline*)**.** A manifold spline of degree k is a triple (M, C, F), where M is the domain manifold with an atlas $\mathscr{A} = \{(U_\alpha, \phi_\alpha)\}$. F is a map $F : M \to \mathbb{R}^3$ representing the entire spline surface. C is the control points set, each control point $\mathbf{c}^I_\beta$ is associated with a set of knots X^I_β which are defined on the domain manifold M directly

$$C := \{\mathbf{c}^I_\beta, X^I_\beta \in M^{|\beta|}, |\beta| = k\}$$

such that

(1) For each chart (U_α, ϕ_α), the restriction of F on U_α is denoted as $F_\alpha = F \circ \phi_\alpha^{-1}$, a subset of control points C_α can be selected from C, such that $(\phi_\alpha(U_\alpha), C_\alpha, F_\alpha)$ form a spline patch of degree k, where $C_\alpha := \{\mathbf{c}^I_\beta, \phi_\alpha(X^I_\beta) \in (\mathbb{R}^2)^{|\beta|}, |\beta| = k\}$.
(2) The evaluation of F is independent of the choice of the local chart, namely, if U_α intersects U_β, then $F_\alpha = F_\beta \circ \phi_{\alpha\beta}$, where $\phi_{\alpha\beta}$ is the chart transition function.

The technical essence of the above definition is to replace a planar domain by the atlas of the domain manifold, and the surface evaluation of the spline patches is independent of the choice of charts (see Fig. 6). After the formal definition, we use one simple example to further illustrate the concept of our manifold splines (see Fig. 7).

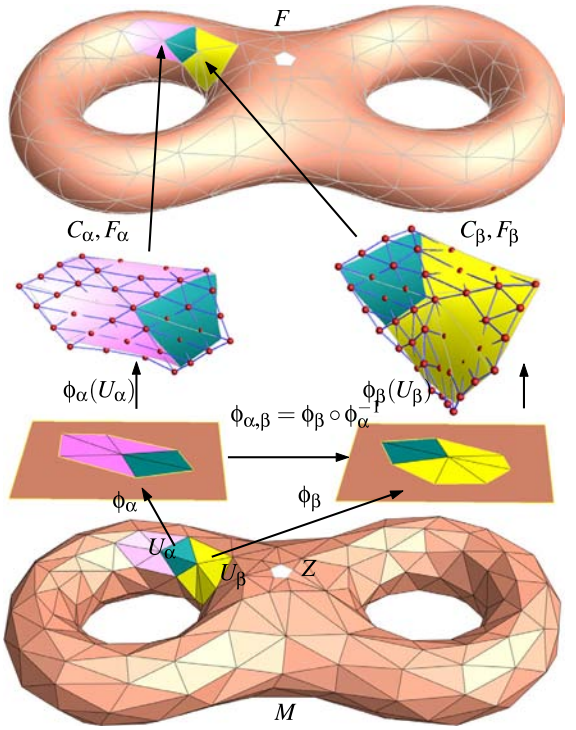

Fig. 6. Key elements of manifold splines: the parametric domain M is a triangular mesh with arbitrary topology as shown at the bottom. The polynomial spline surface F is shown at the top. Two overlapping spline patches $(\phi_\alpha(U_\alpha), C_\alpha, F_\alpha)$ and $(\phi_\beta(U_\beta), C_\beta, F_\beta)$ are magnified and highlighted in the middle. On each parameter chart $(U_\alpha, \phi_\alpha), (U_\beta, \phi_\beta)$, the surface is a triangular B-spline surface. For the overlapping part, its two planar domains differ only by an affine transformation $\phi_{\alpha\beta}$. The zero point neighbor is Z.

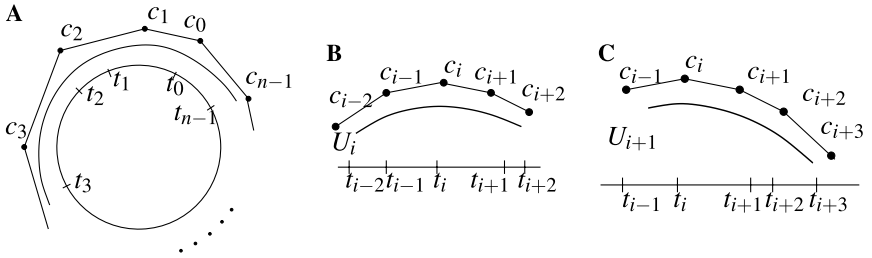

Fig. 7. Manifold splines on S^1: (A) the domain manifold is a unit circle S^1 with n distinct knots $t_0, \ldots, t_{n-1}$; (B) the ith spline patch $U_i = (t_{i-2} - \varepsilon, \ldots, t_{i+2} + \varepsilon)$; (C) the $i+1$th spline patch $U_{i+1} = (t_{i-1} - \varepsilon, \ldots, t_{i+3} + \varepsilon)$.

One Dimensional Example. Here the domain manifold is a unit circle S^1. There are n distinct points $t_0, t_1, \ldots, t_{n-1}$ distributed on the circle in a counterclockwise way. All the summation and subtraction on indices are modular n. The intervals between points are arbitrary. The control net is a planar n-gon, the control points are denoted as $\mathbf{c}_0, \mathbf{c}_1, \ldots, \mathbf{c}_{n-1}$ also in a counterclockwise way, and the knots for c_i are t_{i-2}, t_{i-1}, t_i, t_{i+1}, t_{i+2}.

The affine atlas of S^1 is constructed in the following way: the arc segment $U_i = (t_{i-2} - \varepsilon, t_{i-1}, t_i, t_{i+1}, t_{i+2} + \varepsilon)$, $\varepsilon \in \mathbb{R}^+$ is mapped to an interval in $\mathbb{R}^1$ by $\phi_i : S^1 \to \mathbb{R}^1$, such that

$$\phi_i(t_i) = a, \phi_i(t) = a + b \int_{t_i}^{t} \mathrm{d}s, a \in \mathscr{R}, b \in \mathbb{R}^+. \qquad (6)$$

where a, b are arbitrarily chosen. The union of all local charts (U_i, ϕ_i) form an affine atlas $\mathscr{A} = \{(U_i, \phi_i)\}$. Note that by choosing different a, b, there might be infinite local charts in $\mathscr{A}$.

The control net corresponding to local chart (U_i, ϕ_i) is the line segments $C_i = \{\mathbf{c}_{i-2}, \mathbf{c}_{i-1}, \mathbf{c}_i, \mathbf{c}_{i+1}, \mathbf{c}_{i+2}\}$. The piecewise polynomial curve is formed by n pieces of polynomials, the ith piece $F_i : [t_i, t_{i+1}] \to \mathbb{R}^2$ is evaluated on (U_i, ϕ_i) with control polygon C_i using cubic B-spline.

Then we define the cubic B-spline curve on the unit circle consistently. It is C^2 continuous everywhere. The B-spline patches are $\{\phi_i(U_i), C_i, F_i\}$.

The above example can be trivially extended to construct a two-dimensional surface in a similar way. The key step is to find an affine atlas for the domain manifold. The next section will discuss the existence of such an atlas for general 2-manifolds in detail.

4.2. Equivalence to affine atlas

The central issue of constructing manifold splines is that the atlas must satisfy some special properties to meet all the requirements for the evaluation independence of chart selection. We will show that for a local spline patch, the only admissible parameterizations differ by an affine transformation. This requires that all the chart transition functions are affine.

4.2.1. Admissible parameterizations

From the evaluation process in (4), it is obvious that the only information used there are barycentric coordinates (3) of the parameter with respect to the knots of the control points. If we change the parameter by an affine transformation, the evaluation is invariant and the final shape of the spline surface will not be modified. On the other hand, an affine transformation is the only parametric transformation that will keep the consistency between the spline surface and its parameters. In other words, affine transformations are the only admissible parametric transformations for a spline patch. Note that we present four major theorems as our theoretical results in this section. However, in the interest of technical flow, we defer their proof to Appendix A at the end of this paper.

Theorem 1. *The sufficient and necessary condition for a manifold M to admit manifold spline is that M is an affine manifold.*

This theorem indicates that the existence of manifold splines depends on the existence of affine atlas. If the domain manifold M is an affine manifold, we can easily generalize the planar triangular B-spline surfaces to be defined on M directly. We use the same symbols for manifold spline as in Section 3.1.2. The major differences are as follows:

(1) The knots associated with each vertex $\mathbf{t}_i^I$ in (1) are defined on the manifold directly.

(2) The knots associated with each pole X^I_β in (2) are defined on M directly.
(3) The barycentric coordinates $\lambda^I_{\beta,i}$ used in the evaluation process (3) are defined on any chart of $\mathscr{A}$. Because $\mathscr{A}$ is affine, the value of the barycentric coordinates is independent of the choice of the chart.

4.3. Existence

From the previous discussion, it is clear that in order to define a manifold spline, an affine atlas of the domain manifold must be found first. According to characteristic class theory [28], general closed 2-manifolds do not have an affine atlas. On the other hand, all open surfaces admit an affine atlas. To define manifold splines, the domain manifold has to be modified to admit an atlas by removing a finite number of points. This offers a theoretical evidence to the existence of singular points due to the topological obstruction.

A classical result from characteristic class theory claims that the only closed surface admitting affine atlas is of genus one.

Theorem 2 (Benzécri)**.** *Let S be a closed two dimensional affine manifold, then $\chi(S) = 0$.*

This result is first proven by Benzécri [29]. Shortly after his proof, J. Milnor presented a much more broader result using vector bundle theories [30]. In this framework, the topological obstruction of a global affine atlas is the Euler class. In fact, by removing one point from the closed domain manifold, we can convert it to an affine manifold.

Theorem 3 (*Open surfaces are affine manifold*)**.** *Let M be an orientable open 2-manifold, then M is affine manifold.*

4.4. Spline construction

The existence theorem gives rise to the possibility of generalizing triangular B-splines to manifold domains. Next, we shall present an explicit way to construct affine atlas by utilizing the holomorphic 1-forms of M.

Given a holomorphic 1-form ω on a surface M, assume its zero point set is Z; then, an affine atlas $\mathscr{A}$ for $M\backslash Z$ can be constructed straightforwardly.

Theorem 4 (Affine atlas induced from conformal structure). *Given a closed genus g surface M, and a holomorphic 1-form ω, the zero set of ω is Z, then the size of Z is no more than $2g-2$ and there exists an affine atlas on $M\backslash Z$ deduced by ω.*

4.5. Singular points

Traditional subdivision surfaces, such as Catmull and Clark [31], Doo and Sabin [32], and Loop subdivision [33] surfaces can be considered special cases of manifold splines. The existence of extraordinary points in all subdivision schemes results from their intrinsic topological obstructions. No matter how the domain manifold is remeshed, the extraordinary points can not be entirely removed unless the domain manifold is a torus. Similarly, we can define triangular B-splines on any triangular mesh. If the Euler number of the domain mesh is non-zero, there must be singular points.

Corollary 1 (Existence of singular points)**.** *The manifold splines must have singular points if the domain manifold is closed and not a torus.*

In addition, based on the above discussion, we conclude that the minimal number of extraordinary points is one for all kinds of closed 2-manifolds.

Corollary 2 (Minimal number of singular points)**.** *Given a closed domain 2-manifold, if its Euler number is not zero, a manifold spline can be constructed such that the spline has only one singular point.*

The theoretic results in this section naturally guide us to design practical algorithms to compute affine atlases for arbitrary triangular meshes and subsequently define manifold splines on them.

5. Manifold spline algorithm

This section presents a set of practical algorithms for constructing manifold splines based on triangular B-spline scheme. It is straightforward to define manifold NURBS using similar algorithms.

5.1. Algorithm overview

The major procedures can be summarized as the following main control flow:

Algorithm: construction of manifold splines

(1) Compute a holomorphic 1-form basis for the domain mesh M (Section 5.2).
(2) Select one holomorphic 1-form which optimizes a specified criteria, such as uniformity (see [34]).
(3) Locate zero points of the 1-form (Section 5.3). Remove zero-point neighborhoods, denote the union of zero-point neighborhoods as Z.
(4) Compute the affine atlas for $M\backslash Z$ (Section 5.4).
(5) Assign knots for each control point (Section 5.5).
(6) Evaluate the spline surface (Section 5.6).

5.2. Holomorphic 1-form

The algorithm for computing the holomorphic 1-form for a triangular mesh is as follows:

Algorithm: compute holomorphic one form

(1) Compute the first homology group basis of the domain manifold M, $H_1(M,\mathbb{Z})$.
(2) Compute the first cohomology group basis of the domain manifold M, $H^1(M,\mathbb{R})$.
(3) Compute harmonic 1-form basis from $H^1(M,\mathbb{R})$ using heat flow method.
(4) For each harmonic 1-form basis ω_x, locally rotate by a right angle about the normal to get ω_y (Hodge star operator), pair (ω_x,ω_y) to form a holomorphic 1-form basis.

The computation process is equivalent to solving an elliptic partial differential equation on the surface using finite element method. The details for computing holomorphic 1-form are thoroughly explained in [26,27].

5.3. Locating singular points

If the resolution of a mesh is high enough, the holomorphic 1-form is accurate enough to locate the zero points automatically.

Using the holomorphic 1-form, the neighborhood of the zero point will be mapped to a planar region. The behavior of the map is similar to the map $z \to z^2,\ z \in \mathbb{C}$ in the neighborhood of the origin. More rigorously, a circle around the zero point will be mapped to a curve which passes around the origin at least twice. (The winding number of the image curve about the origin is no less than 2.)

The following algorithm aims to locate zero points:

Algorithm: locate zero points

(1) Given a vertex $v \in M$, a holomorphic 1-form ω, find all the vertices connecting to vertex v sorted counterclock-wisely, denoted as $w_0, w_1, \ldots, w_{n-1}$.
(2) Map w_i to the plane using ω, $\phi(w_i) = \int_v^{w_i} \omega$.
(3) The points $\phi(w_0), \phi(w_1), \ldots, \phi(w_{n-1})$ form a planar polygon and the point $\phi(v)$ is inside this polygon. Compute the summation of the angles

$$\sum_{i=0}^{n-1} \angle\phi(w_i)\phi(v)\phi(w_{i+1}),$$

where $w_n = w_0$. If this summation is 2π, then v is a regular point; if summation is no less than 4π, then v is a zero point.

5.4. Constructing affine atlas

An affine atlas can be constructed in the following way:

Algorithm: construct affine atlas

(1) Locate zero points of ω, denote the zero points Z.
(2) Remove zero points and the faces attaching to them.
(3) Construct an open covering for $M\backslash Z$. For each vertex, take the union of all faces within its k-ring neighbor as an open set U.
(4) Test if the union of any two U_α, U_β is a topological disk by checking the Euler number of $U_\alpha \cup U_\beta$. If not, subdivide U_α.
(5) Pick one vertex $p_\alpha \in U_\alpha$, for any vertex $p \in U_\alpha$, define $\phi_\alpha(p) = \int_{p_\alpha}^{p} \omega$.
(6) Compute coordinate transition functions, $\phi_{\alpha\beta} = \int_{p_\alpha}^{p_\beta} \omega$.

5.5. Assigning knots

The connectivity of the control net can be easily determined by the uniform subdivision of the domain mesh. For example, if the desired spline

surface is quadratic, each face on M will be subdivided to four faces on the control net. Therefore, each face on the control mesh is covered by one face on M. Each control point will then associate with a group of knots. The knots are defined in the following way:

Algorithm: assign knots

(1) Given a control point $c \in C$ and a face f attached to c. Suppose f is covered by $F \in M$. Choose one local chart (U_α, ϕ_α) covering F, and assign knots X^F_β to c in this local chart.
(2) Record the chart id α, the knots X^F_β for c.

5.6. Surface evaluation

As explained above, the evaluation process is independent of the choice of the chart. The chart can be chosen arbitrarily, and all associated knots must then be converted to the selected chart.

Algorithm: spline evaluation

(1) Choose a face F on M, choose a coordinate chart (U_α, ϕ_α) covering F.
(2) Locate all control points associate with F.
(3) If the knots of a control point c is define on coordinate chart β, then convert the knots to chart (U_α, ϕ_α) using transition function $\phi_{\beta\alpha}$.
(4) Evaluate the polynomial surface using the evaluation algorithm for B-spline surface with planar domain on (U_α, ϕ_α).

6. Implementation and experimental results

In our implementation, we consider domain manifolds represented as triangular meshes M. We use v_k to denote the vertices of M, $[v_i, v_j]$ denote the oriented edge from v_i to v_j $[v_i, v_j, v_k]$ to denote an oriented face of M.

6.1. Data structure

The primary data structures in our prototype system for constructing manifold splines are *domain mesh M*, *control net C*, *affine atlas* $\mathscr{A}$, and *holomorphic 1-form* ω.

Domain mesh M. The domain mesh in general is a triangular mesh, represented by a half-edge data structure. Each face is covered by several coordinate charts.

Control net C. The control net is also a triangular mesh, represented by half edge data structure. The connectivity of the control net is deduced from that of the domain mesh by uniform subdivision and the degree of the manifold spline. Each face on the control net corresponds to one covering face in the domain mesh.

Atlas $\mathscr{A}$. The atlas is set of charts and all the transition functions among them. The transition functions are translations on the plane; if the αth chart and the βth chart intersect, there is a transition function $\phi_{\alpha\beta}$, represented as a translation vector in $\mathbb{R}^2$. Each chart is a set of adjacent faces, which form a topological disk. We ensure that the union of two intersecting charts is still a topological disk. The local coordinates are not recorded, but computed in real-time by integrating holomorphic 1-form ω.

Holomorphic 1-form ω. A holomorphic 1-form is represented by a map from the oriented edge (half-edge) set of M to $\mathbb{R}^2$, $\omega : E \to \mathbb{R}^2$, such that for any face $[v_0, v_1, v_2]$

$$\omega[v_0, v_1] + \omega[v_1, v_2] + \omega[v_2, v_0] = 0.$$

6.2. Experimental results

Our prototype system is implemented in C++ on Windows platform. We build a complete system for computing topological structure, conformal structure, and affine structure. The system is based on a half-edge data structure, and uses the finite element method to solve elliptic partial differential equations on surfaces. The system includes traditional mesh processing functionalities, such as mesh simplification, subdivision, smoothing, and progressive mesh algorithms. But the main functionalities of the system are computing the homology group, cohomology group, harmonic 1-forms, holomorphic 1-forms, global conformal parameterizations, manifold spline construction, and surface evaluation.

Table 2 summarizes our experiment results. Fig. 8 illustrates the process of our manifold spline by constructing a manifold spline on a genus 2 surface. Fig. 11 shows several examples of manifold splines of various topological type. The results prove both the theoretic rigor and feasibility in practice.

Table 2
Spline configurations: g, genus; n, degree; N_b, No. of boundaries; N_s, No. of singular points; N_t, No. of domain triangles; N_c, No. of control points

Object	Figure	g	N_b	N_s	n	N_t	N_c
Bunny	Fig. 9	0	3	1	3	293	1348
Knot	Fig. 11, row 1	1	0	0	3	400	1800
Rockerarm	Fig. 11, row 2	1	0	0	3	2125	9676
Two-hole torus	Fig. 8	2	0	2	3	502	2270
Sculpture	Fig. 11, rows 3 and 4	3	0	4	3	1458	6583

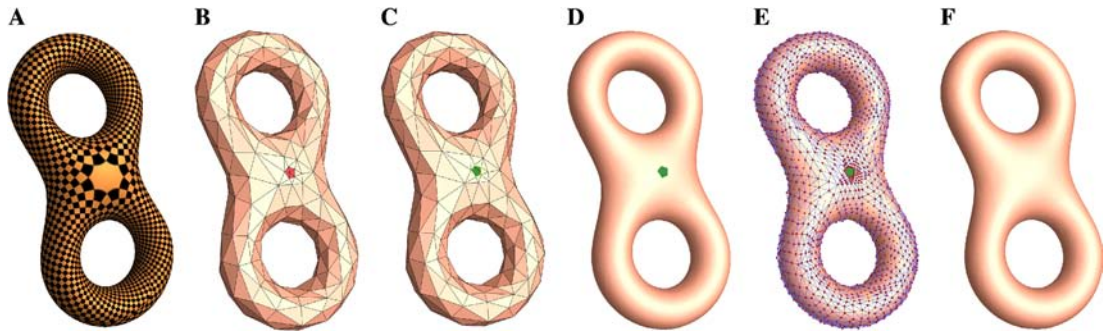

Fig. 8. Construction of manifold spline: (A) Holomorphic 1-form ω, the octagonal region indicates a singular point; (B) Domain manifold M; (C) singular point removal $M\backslash Z$; (D) Manifold spline F; (E) spline surface F covered by control net C; (F) the regions of singular points are filled.

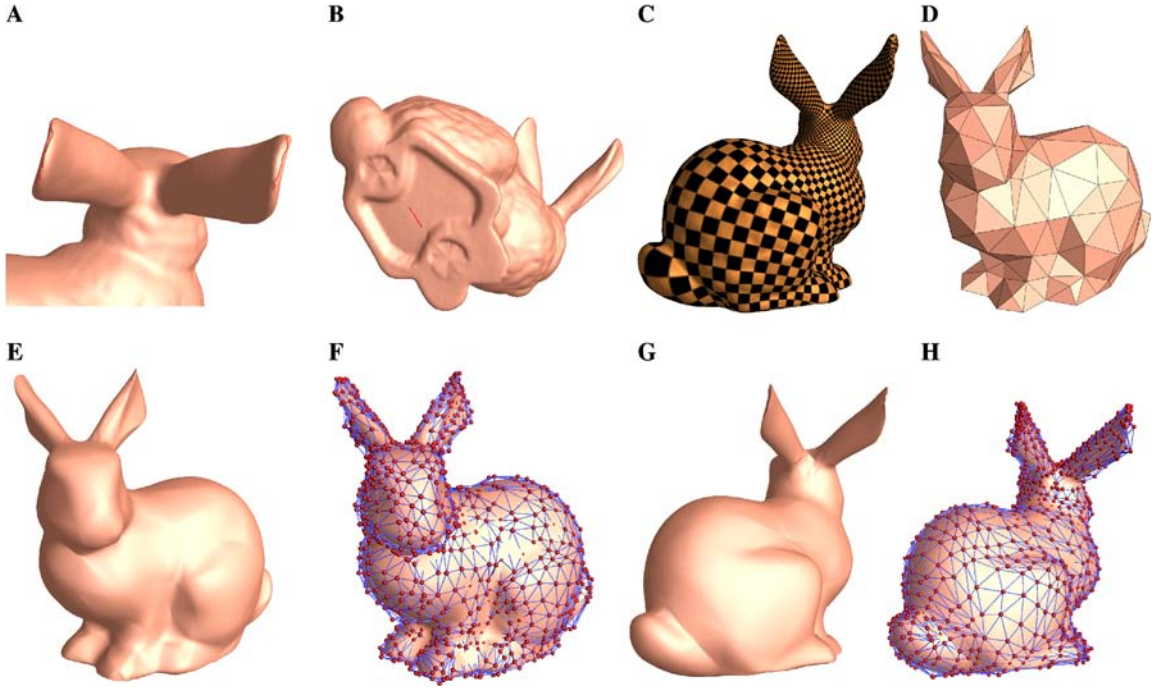

Fig. 9. Genus zero manifold spline: (A and B) the topological modification by introducing three boundaries marked as red curves. The genus of the double covered surface is two. (C) The holomorphic 1-form ω. By projecting the holomorphic 1-form of the double covered mesh to the original surface, there is only one singular point, which is on the top of the bunny head. (D) The domain manifold M; (E and F) the front view of polynomial surface F and control net C; (G and H) show the back view of polynomial surface F and control net C. (For interpretation of the references to colour in this figure legend, the reader is referred to the web version of this paper.)

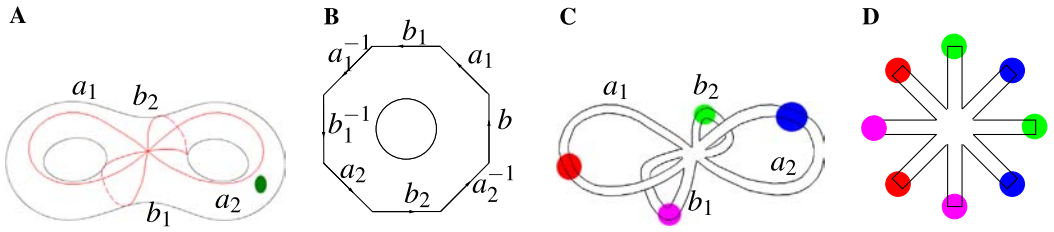

Fig. 10. Open surfaces are affine manifolds: An genus 2 surface M with one boundary in (A) is isomorphic to an octagon with a hole in (B), then the octagon is immersed in $\mathbb{R}^2$ as the ribbon figure in (C). The colored disks indicate the open sets U_α of M. There is another open set U, which covers $M \setminus \cup U_\alpha$. U and U_α are mapped to $\mathbb{R}^2$ as shown in (D). All transitions are rotation and translation. This illustrates the affine atlas for the open surface of M. (For interpretation of the references to colour in this figure legend, the reader is referred to the web version of this paper.)

7. Conclusion

We have proved in this paper that defining triangular B-splines over arbitrary manifolds is equivalent to the existence of an affine atlas of the underlying manifold. In addition, we have articulated a systematic way to construct an affine atlas for general manifolds and developed a suite of algorithms that enable the definition and computation of triangular B-splines over any manifold domain (consisting of general meshes). Our theoretical and algorithmic contribution to the field of solid and physical modeling is a general framework that extends spline surfaces with planar domains to manifold splines, which are piecewise polynomials defined over arbitrary manifold. Because of the intrinsic topological obstruction for any manifold, singular points are unavoidable. We utilize the concept and computational techniques of Riemann surface theory (especially the holomorphic 1-forms) to obtain the affine atlas and minimize the number of singular points for our manifold splines simultaneously. The prototype software and experimental results have demonstrated the great potential of our manifold splines in shape modeling, geometric design, graphics, and engineering applications.

At present, we are planning to pursue several directions as future work. First, the behavior of singular points is not yet known. We shall seek new mathematical tools for the rigorous analysis of singular points. Second, we shall investigate other new spline schemes and explore their manifold generalizations.

Acknowledgments

The authors thank the reviewers for their careful review and helpful suggestions. This work was partially supported by the NSF CAREER Award CCF-0448339 to X. Gu and the NSF Grant ACI-0328930, the ITR Grant IIS-0326388, and Alfred P. Sloan Fellowship to H. Qin.

Appendix A

We present the detailed proof of our major theoretic results in the Appendix.

Lemma 1.1. *Assume there are two spline surface patches of C^k continuity, $k > 0$*

$S = (U, C, F)$ and $\tilde{S} = (\tilde{U}, \tilde{C}, \tilde{F})$.

The parametric transformation

$\phi : U \to \tilde{U}$

is invertible. Suppose $S, \tilde{S}$ share the same knot configuration, namely, the triangulation $\tilde{\mathcal{T}}$ is induced from $\mathcal{T}$ by ϕ, and the knots $\tilde{t}^I_{i,j}$ are induced from $t^I_{i,j}$ by ϕ

$$\tilde{t}^I_{i,j} = \phi(t^I_{i,j}), \tag{7}$$

the control points with corresponding knots coincide $\mathbf{c}^I_\beta = \tilde{\mathbf{c}}^I_\beta$, then

(1) if ϕ is affine, then $F = \tilde{F} \circ \phi$ holds for arbitrary control nets.
(2) if $F = \tilde{F} \circ \phi$ holds for arbitrary control nets, then ϕ is affine.

In other words, the following diagram commutes for arbitrary control nets

$$\begin{array}{ccc} U \subset \mathbb{R}^2 & \xrightarrow{\phi} & \tilde{U} \subset \mathbb{R}^2 \\ \downarrow F & & \downarrow \tilde{F} \\ F(U) \subset \mathbb{R}^3 & \xrightarrow[id]{} & \tilde{F}(\tilde{U}) \subset \mathbb{R}^3 \end{array} \tag{8}$$

if and only if ϕ is affine.

Fig. 11. Manifold spline examples: (A) Holomorphic 1-form ω which induces the affine atlas $\mathscr{A}$; (B) parametric domain manifold M with singular points Z marked; (C) Polynomial spline F defined on the manifold M in (A); (D) the red curves on spline F correspond to the edges in the domain manifold M; (E) spline F covered by control net C. (For interpretation of the references to colour in this figure legend, the reader is referred to the web version of this paper.)

Proof. The sufficient condition part is obvious, because the evaluation of the splines only involves barycentric coordinates. Affine transformations preserve the barycentric coordinates; therefore the diagram is commutative.

The proof for the necessary condition requires the completeness of the spline scheme 3. We set all control points of C to be zero except the one corresponding to knots X^I_β. Correspondingly, we set all control points of $\tilde{C}$ to be zero except one corresponding to knots $\tilde{X}^I_\beta$. Then we get the basis functions $F(\mathbf{u}) = N^I_\beta(\mathbf{u})$, $\tilde{F} = \tilde{N}^I_\beta(\tilde{\mathbf{u}})$, by $F = \tilde{F} \circ \phi$, we get

$$N^I_\beta(\mathbf{u}) = \tilde{N}^I_\beta(\tilde{\mathbf{u}}).$$

Therefore, all basis functions of S equal the corresponding basis functions of $\tilde{S}$. Suppose $\mathbf{u} = (u_1, u_2)$, then u_1 is a polynomial of (u_1, u_2). By completeness of the spline scheme, u_1 can be represented as the linear combination of $N^I_\beta(\mathbf{u})$, therefore it can be represented as the linear combination of $\tilde{N}^I_\beta(\tilde{\mathbf{u}})$. As a result, u_1 and u_2 can be represented as piecewise polynomials of $\tilde{\mathbf{u}}$ of C^k continuity. Because S and $\tilde{S}$ are symmetric, $\tilde{\mathbf{u}}$ are also piecewise polynomials of $\mathbf{u}$ of C^k continuity. Therefore, u and $\tilde{\mathbf{u}}$ can linearly represent each other piecewisely with C^k continuity. So, because the parameter transition ϕ is piecewise linear and C^k continuous, ϕ must be a global linear map over all pieces. In other words, ϕ is affine. □

Theorem 1. *The sufficient and necessary condition for a manifold M to admit manifold spline is that M is an affine manifold.*

Proof. Consider two intersecting local charts (U_α, ϕ_α) and (U_β, ϕ_β), where the manifold spline F restricted on them are F_α and F_β, respectively. We select a subset of control points C whose knots are contained in $U_\alpha \cap U_\beta$. The spline patches $(\phi_\alpha(U_\alpha \cap U_\beta), C, F_\alpha)$ and $(\phi_\beta(U_\alpha \cap U_\beta), C, F_\beta)$ satisfy the condition in Lemma 1, therefore, the chart transition function $\phi_{\alpha\beta}$ must be affine. □

Theorem 2 (*Benzécri*)**.** *Let S be a closed two dimensional affine manifold, then $\chi(S) = 0$.*

The proof for this classical result can be found in Benzécri's work [29,35]. Milnor used vector bundle theories to prove it in [30,36].

Theorem 3 (Open surfaces are affine manifold)**.** *Let M be an orientable open 2-manifold, then M is an affine manifold.*

Proof. Fig. 10 illustrates the proof by constructing an affine atlas for the open surface M in (a). One boundary may be a closed curve or a single point as shown in (a) by a dark spot. We deform (a) continuously to generate (b) by gradually enlarging the hole. (b) is homeomorphic to the ribbon figure in (c), which is immersed in $\mathbb{R}^2$. Then we cut each annulus of (c) to get a fundamental domain as shown in (d).

The colored disks U_α are open sets of M, another open set U can be defined to cover $M \setminus \cup U_\alpha$. (d) The way U and U_α's are mapped to $\mathbb{R}^2$. It is obvious that all chart transition functions are combinations of translations and rotations.

For surfaces with multiple boundaries, we can fill all of the boundaries with disks except one, and the proof is similar.

Theorem 4 (Affine atlas induced from conformal structure)**.** *Given a closed genus g surface M, a holomorphic 1-form ω. The zero set of ω is Z, then the size of Z is no more than $2g-2$ and there exists an affine atlas on $M \setminus Z$ deduced by ω.*

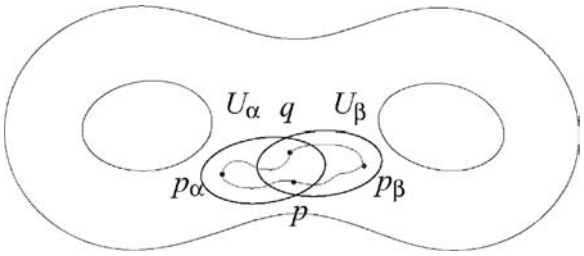

Proof. The existence and the number of zero points Z of the holomorphic 1-form ω can be proved using Riemann–Roch theorem [25] or Poicaré–Hopf theorem. Because $\omega = \omega_x + i\omega_y$ is holomorphic, ω_x is a harmonic 1-form. Since we treat ω_x as a vector field, the singularities can only have negative indices, and the summation of their indices equals the Euler number $2-2g$. Hence, the geometric number of zero points is no more than $2g-2$.

Suppose an open covering of $M \setminus Z$ is a collection of open sets $\{U_0, U_1, \ldots,\}$. We require that if two open sets U_α, U_β intersect each other, $U_\alpha \cap U_\beta \neq \phi$, then their union $U_\alpha \cup U_\beta$ is a topological disk (see Fig. 7). If this requirement can not be satisfied, we can subdivide the open sets until the requirement is met. Then we select one point in each U_α, denoted as $p_\alpha \in U_\alpha$, for any point $p \in U_\alpha$, we define the coordinate of p as

$$\phi_\alpha(p) = \int_{p_\alpha}^{p} \omega,$$

where the path from p_α to p is arbitrarily chosen. Then we claim $\mathscr{A} = \{(U_\alpha, \phi_\alpha)\}$ is an affine atlas for $M \setminus Z$.

We want to show for any $p \in U_\alpha \cap U_\beta$, $\phi_\beta(p) = \phi_\alpha(p) + \text{const}$, namely, the coordinate transition function $\phi_{\alpha\beta} : \mathbb{R}^2 \to \mathbb{R}^2$ is a translation. Suppose $p, q \in U_\alpha \cap U_\beta$ as shown in the above figure

$$\begin{aligned}(\phi_\beta(p) - \phi_\alpha(p)) - (\phi_\beta(q) - \phi_\alpha(q)) \\ = \int_{p_\beta}^{p} \omega - \int_{p_\alpha}^{p} \omega - \int_{p_\beta}^{q} \omega + \int_{p_\alpha}^{q} \omega, \end{aligned} \tag{9}$$

Because $U_\alpha \cup U_\beta$ is a topological disk, the closed curve $r = p_\beta \to p \to p_\alpha \to q \to p_\beta$ is homotopic to zero. Because the curlex of both ω_x and ω_y are zeros, the above integration is zero, $\oint_r \omega = 0$. There-

fore $\phi_\beta(p) - \phi_\alpha(p) \equiv const$ for arbitrary $p \in U_\alpha \cap U_\beta$, the transition function $\phi_{\alpha\beta}$ is a translation. □

References

[1] M. Eck, H. Hoppe, Automatic reconstruction of *B*-spline surfaces of arbitrary topological type, in: Proceedings of SIGGRAPH '96, 1996, pp. 325–334.

[2] C. de Boor, Splines as linear combinations of *B*-splines. A surveyApproximation Theory II, Academic Press, New York, 1976, pp. 1–47.

[3] W. Dahmen, C.A. Micchelli, H.-P. Seidel, Blossoming begets *B*-spline bases built better by *B*-patches, Math. Comput. 5 (199) (1992) 97–115.

[4] P. Fong, H.-P. Seidel, Control points for multivariate *B*-spline surfaces over arbitrary triangulations, Comput. Graphics Forum 1 (4) (1991) 309–317.

[5] G. Greiner, H.-P. Seidel, Modeling with triangular *B*-splines, IEEE Comput. Graph. Appl. 1 (2) (1994) 56–60.

[6] R. Pfeifle, H.-P. Seidel, Fitting triangular *B*-splines to functional scattered data, in: Graphics Interface '95, 1995, pp. 26–33.

[7] M. Franssen, R.C. Veltkamp, W. Wesselink, Efficient evaluation of triangular *B*-spline surfaces, Computer-Aided Geom. Design 1 (9) (2000) 863–877.

[8] M. Neamtu, Bivariate simplex *B*-splines: a new paradigm, in: SCCG '01: Proceedings of the 17th Spring conference on Computer graphics, 2001, pp. 71–78.

[9] Y. He, X. Gu, H. Qin, Fairing triangular *B*-splines of arbitrary topology, in: Proceedings of Pacific Graphics '05 (short paper), 2005, pp. 153–156.

[10] P. Alfeld, M. Neamtu, L.L. Schumaker, Bernstein–Bezier polynomials on spheres and sphere-like surfaces, Computer-Aided Geom. Design 1 (4) (1996) 333–349.

[11] P. Alfeld, M. Neamtu, L.L. Schumaker, Fitting scattered data on sphere-like surfaces using spherical splines, J. Comput. Appl. Math. 7 (1–2) (1996) 5–43.

[12] R. Pfeifle, H.-P. Seidel, Spherical triangular *B*-splines with application to data fitting, Comput. Graph. Forum 1 (3) (1995) 89–96.

[13] M. Neamtu, Homogeneous simplex splines, J. Comput. Appl. Math. 7 (1-2) (1996) 173–189.

[14] Y. He, X. Gu, H. Qin, Rational spherical splines for genus zero shape modeling, in: Proceedings of Shape Modeling International '05, 2005, pp. 82–91.

[15] C.M. Grimm, J.F. Hughes, Modeling surfaces of arbitrary topology using manifoldsProceedings of ACM SIGGRAPH '95, ACM Press, 1995, pp. 359–368.

[16] Yu. K. Demjanovich, Finite-element approximation on manifolds, in: Proceedings of the International Conference on the Optimization of the Finite Element Approximations (St. Petersburg, 1995), vol. 8, 1996, pp. 25–30.

[17] J. Cotrina, N. Pla, Modeling surfaces from meshes of arbitrary topology, Computer-Aided Geom. Design 1 (7) (2000) 643–671.

[18] J. Cotrina, N. Pla, M. Vigo, A generic approach to free form surface generation, in: Proceedings of the Seventh ACM Symposium on Solid Modeling and Applications, 2002, pp. 35–44.

[19] Lexing Ying, D. Zorin, A simple manifold-based construction of surfaces of arbitrary smoothness, ACM Trans. Graph. 2 (3) (2004) 271–275.

[20] J. Wallner, H. Pottmann, Spline orbifolds, Curves Surfaces Appl. CAGD (1997) 445–464.

[21] L. Ramshaw, Blossoming: a connected-the-dots approach to splines, Technical Report, Digital Systems Research Center, Palo Alto, 1987.

[22] L. Ramshaw, Blossom are polar forms, Computer-Aided Geom. Design 6 (4) (1989) 323–358.

[23] H.-P. Seidel, Polar forms and triangular *B*-spline surfaces, in: D.-Z. Du, F. Hwang (Eds.), second ed., Euclidean Geometry and Computers, World Scientific Publishing, Singapore, 1994, pp. 235–286.

[24] Raúl Gormaz, *B*-spline knot-line elimination and Bézier continuity conditions, in: Curves and Surfaces in Geometric Design, A K Peters, Wellesley, MA, 1994, pp. 209–216.

[25] J. Jost, R.R. Simha, Compact Riemann Surfaces: An Introduction to Contemporary Mathematics, Springer-Verlag Telos, 1997.

[26] Xianfeng Gu, Shing-Tung Yau, Computing conformal structures of surfaces, Commun. Inform. Syst. 2 (2) (2002) 121–146.

[27] Xianfeng Gu, Shing-Tung Yau, Global conformal surface parameterization, in: Proceedings of the Eurographics/ACM SIGGRAPH Symposium on Geometry Processing, 2003, pp. 127–137.

[28] J.W. Milnor, J.D. Stasheff, Characteristic Classes, Princeton University Press, 1974.

[29] J.P. Benzécri, Variétés localement affines, Sem. Topologie et Géom. Diff., Ch. Ehresmann (1958–1960) (7) (1959).

[30] J.W. Milnor, On the existence of a connection with curvature zero, Commun. Math. Helv. 32 (1958) 215–223.

[31] E. Catmull, J. Clark, Recursively generated *B*-spline surfaces on arbitrary topological meshes, Computer-Aided Design 1 (6) (1978) 350–355.

[32] D. Doo, M. Sabin, Behaviour of recursive division surfaces near extraordinary points, Computer-Aided Design 1 (6) (1978) 356–360.

[33] C. Loop, Smooth subdivision surfaces based on triangles, Master's thesis, University of Utah, Dept. of Mathematics, 1987.

[34] M. Jin, Y. Wang, S.-T. Yau, X. Gu, Optimal global conformal surface parameterization, in: Proceedings of IEEE Visualization, 2004, pp. 267–274.

[35] J.P. Benzécri, Sur les variétés localement affines et projectives, Bull. Soc. Math. France 88 (1960) 229–332.

[36] J.W. Milnor, On fundamental groups of complete affinely flat manifolds, Adv. Math. 25 (1977) 178–187.